Perspective

The Bending Mode of Water: A Powerful Probe for Hydrogen Bond Structure of Aqueous Systems

Takakazu Seki,[#] Kuo-Yang Chiang,[#] Chun-Chieh Yu, Xiaoqing Yu, Masanari Okuno, Johannes Hunger, Yuki Nagata,* and Mischa Bonn*

Read Online

ACCESS | ⭲ Metrics & More | 🔳 Article Recommendations

ABSTRACT: Insights into the microscopic structure and dynamics of the water's hydrogen-bonded network are crucial to understand the role of water in biology, atmospheric and geochemical processes, and chemical reactions in aqueous systems. Vibrational spectroscopy of water has provided many such insights, in particular using the O−H stretch mode. In this Perspective, we summarize our recent studies that have revealed that the H−O−H bending mode can be an equally powerful reporter for the microscopic structure of water and provides more direct access to the hydrogen-bonded network than the conventionally studied O−H stretch mode. We discuss the fundamental vibrational properties of the water bending mode, such as the intermolecular vibrational coupling, and its effects on the spectral lineshapes and vibrational dynamics. Several examples of static and ultrafast bending mode spectroscopy illustrate how the water bending mode provides an excellent window on the microscopic structure of both bulk and interfacial water.
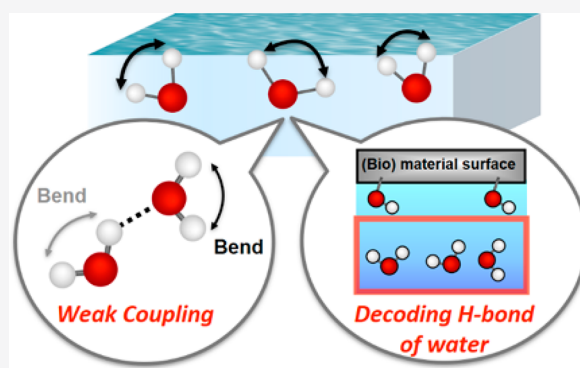
Water plays an important role in many biological and chemical processes. The hydration structure of proteins and lipids affects their biological functions, and the interaction of water with solid surfaces such as mineral and metal oxide surfaces determines surface chemistry and surface−catalytic reactions. In addition to these critical roles in natural and industrial processes, the fundamental physical properties of condensed phase (liquid- and solid-state bulk water) and interfacial water, e.g., anomalously high surface tension, high viscosity, high boiling point, and so forth, have also attracted a great deal of attention. Some of these unique features have been attributed to the cooperative hydrogen-bond network of multiple water molecules.[1] Thus, to unveil the physics underlying the unique properties of water, a molecular-level understanding of the structure and dynamics of the hydrogen-bond network is essential.

Vibrational spectroscopy techniques have provided detailed information on the microscopic hydrogen-bond structure of water in aqueous solutions, primarily via the O−H stretch mode of water.[2,3] The study of the O−H stretch mode is prompted by the strong correlation between the frequency of O−H stretch vibration and the individual hydrogen-bond strength (Figure 1a);[4,5] a strong (weak) hydrogen bond leads to a red-shift (blue-shift) of the O−H stretch frequency. While the O−H stretch frequency is an excellent marker of the local hydrogen-bonding arrangement in neat water or very simple systems, complications quickly arise when other molecular
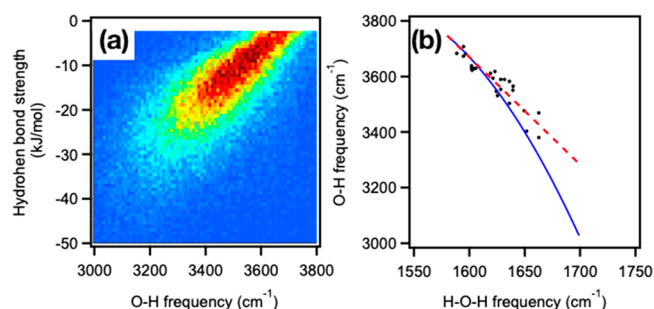

Figure 1. (a) Time averaged probability distribution of the O−H stretch frequency vs hydrogen bond strength. Reproduced from ref 5. (b) A scatter plot of the experimentally determined H−O−H bending frequency vs averaged O−H stretch frequency of water. The data points were experimentally obtained by measuring the frequencies of water in various media.[6] The blue and red lines represent the relations of eqs 1 and 2, respectively.
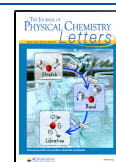
moieties are present in the sample. The broad O−H stretch band of water then overlaps with other vibrational bands such as the O−H stretch mode of alcohols and biomolecules as well as their N−H stretch/amide A modes. Disentangling the different modes is a formidable challenge, which cannot be resolved, for instance, by H/D isotopic substitution, because of rapid proton exchange. Also, vibrational couplings such as energy splitting between the O−H stretch modes and Fermi resonance with bending overtone often complicate the interpretation of the O−H stretch mode spectra and dynamics.

Compared to the stretch mode, the H−O−H bending mode has several advantages. Because the bending mode of water is unique to water molecules, it is spectrally separated from the C−O−H and C−N−H bending modes of alcohols and biomolecules. Essentially, water has only one bending mode in a molecule, which means there is no intramolecular bending mode−bending mode vibrational coupling. In addition to these advantages, the bending frequency can provide information on the hydrogen-bond strength of water, in a manner very similar to the stretch mode frequency. For example, the bending mode frequency of the H−O−H increases from ~1590 cm^{-1} in the gas phase to ~1650 cm^{-1} in the liquid phase because of the formation of hydrogen bonds. More quantitatively, Falk proposed the linear relation of the O−H stretch mode frequency and H−O−H bending mode frequency (Figure 1b), which satisfies the stretch and bend frequencies in the gas phase ($\omega^{\text{g}}_{\text{bend}} = 1590.4$ cm^{-1} and $\omega^{\text{g}}_{\text{str}} = 3706$ cm^{-1}). This reads[6]

$$\omega^{\text{g}}_{\text{str}} - \omega_{\text{str}} = -\frac{(\omega^{\text{g}}_{\text{bend}} - \omega_{\text{bend}})}{0.2583} \quad (1)$$

A very similar coefficient of $-1/0.259$ was obtained from *ab initio* calculations.[7] When the nonlinear term is included in eq 1, one can add the additional condition satisfying the stretch and bend frequencies in liquid water ($\omega^{\text{l}}_{\text{bend}} = 1650$ cm^{-1} and $\omega^{\text{l}}_{\text{str}} = 3400$ cm^{-1}) to eq 1.[8,9] This is given as[10]

$$\omega^{\text{g}}_{\text{str}} - \omega_{\text{str}} = -\frac{(\omega^{\text{g}}_{\text{bend}} - \omega_{\text{bend}})}{0.2583} + 0.0216$$
$$\times (\omega^{\text{g}}_{\text{bend}} - \omega_{\text{bend}})^2 \quad (2)$$

These relations manifest that the higher H−O−H bending mode frequency indicates the lower O−H stretch mode frequency, thus indicative of a stronger intermolecular O··H hydrogen-bond.

> The H−O−H bending mode frequency is responsive to the hydrogen-bond strength of the system of interest.

The vibrational nature of the water bending mode, however, has been much less investigated than the stretch mode, presumably because of its weaker absorbance. In contrast to the O−H stretch mode, it has been unclear how isotopic dilution affects the spectral shape and the vibrational dynamics of the bending mode, i.e., bending mode−bending mode and bending mode−other vibrational mode couplings have not been fully elucidated.[2] At the interface, it has been controversially discussed whether the bending mode signal in surface-specific vibrational spectra arises from the interfacial water molecules[7,11,12] or from the bulk.[13] As such, despite the

potential advantage of using the bending mode probe to explore the hydrogen-bond network, fundamental knowledge on the vibrational nature of the bending mode is still lacking.

In this Perspective, recent spectroscopic advances on the water bending mode will be introduced, followed by a discussion of the fundamental vibrational properties of the bending mode in bulk liquid, the vibrational dynamics, and the surface specificity and coupling nature of the bending mode of the interfacial water. Subsequently, several examples of probing the bending mode of water are discussed. Finally, the key results are summarized.

First, we examined the static spectra of the water bending mode in pure bulk water through the comparison of the stretch and the bending modes. Figure 2a shows that the use of isotopically diluted water (HOD in D$_2$O) changes the lineshapes of the O−H stretch mode in both the IR and Raman spectra of neat H$_2$O.[14,15] The shoulder at ~3200 cm^{-1} diminishes while the ~3400 cm^{-1} contribution persists upon isotopic dilution, resulting in an overall narrowing of the vibrational line shape. These spectral variations are well reproduced by simulations using the frequency-mapping technique (Figure 2b) and can be explained by intermolecular intramode (i.e., stretch mode−stretch mode) coupling as well as intramolecular intermode coupling mainly due to the Fermi resonance between the stretch and the overtone of the bending mode.[16,17] The intra/intermolecular intra/inter-mode couplings for the O−H stretch mode and H−O−H bending mode are summarized in Tables 1 and 2, respectively.

How does the lineshape of the bending mode change upon isotopic dilution of water? Recently, we compared the experimentally determined lineshapes of the H−O−H bending mode of neat H$_2$O and isotopically diluted water by carefully subtracting the H−O−D bending mode contribution from the measured spectra, which is plotted in Figure 2c.[18] The data show that the peak frequency is slightly shifted to higher frequencies (~7 cm^{-1}) upon isotopic dilution. At the same time, the full width at half-maximum (fwhm) of the bending mode is rather insensitive to the isotopic composition, in stark contrast to the stretch mode. Modeling and detailed analysis of bending mode spectra are, however, still largely unexplored. One of the pioneering works for the bending mode has been reported by Ni and Skinner.[7] Figure 2d displays the simulated bending mode IR spectra with and without the intermolecular intramode (bending mode−bending mode) coupling. Figure 2d shows a slight blue-shift (~10 cm^{-1}) of the uncoupled oscillators, relative to the coupled mode, in reasonable agreement with the experimental data.[18] However, the simulation indicates a substantial narrowing of the H−O−H bending mode spectra upon isotopic dilution, in contrast to the experimental spectra in Figure 2c. As such, theoretical modeling of the IR bending mode spectra is challenging. Furthermore, a theoretical calculation of the Raman response of the bending mode is lacking.

Overall, the experimental lineshapes indicate that intermolecular intramode coupling of the bending mode causes only minimal distortion of the lineshape, and shifts the peak position of the bending mode spectra of water, but the shift is very tiny. This is in contrast with the stretch mode response, which is strongly affected by a complex interplay of intramolecular intermode and intermolecular intramode couplings. Thus, the water bending mode in bulk water is a more direct reporter of the hydrogen-bond network.
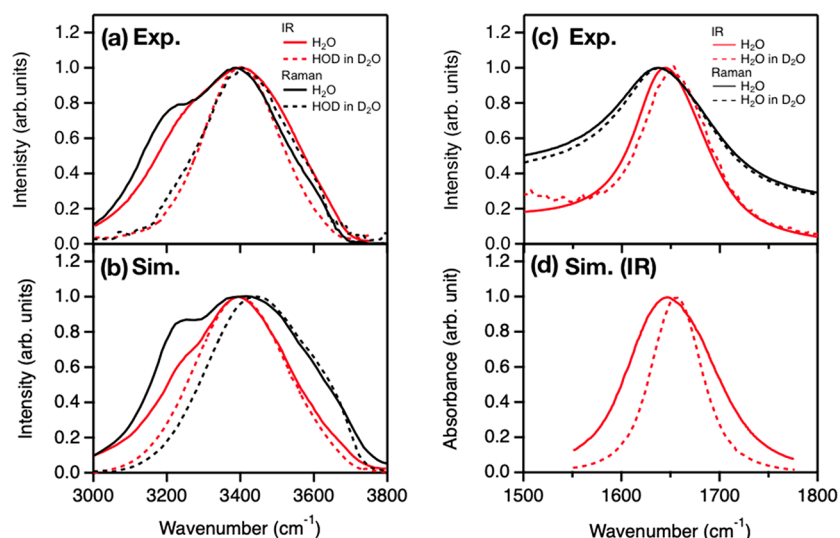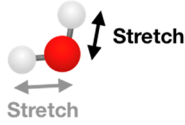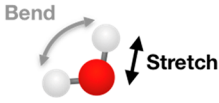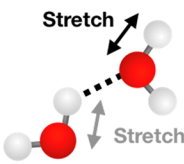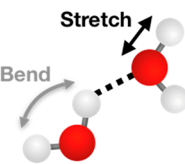
Figure 2. (a) Measured IR and Raman spectra of the O−H stretch vibration. The data are reproduced from refs 14 and 15, respectively. (b) Computed IR and Raman spectra of the O−H stretch vibration based on the frequency-mapping technique, with the intermolecular intramode coupling and Fermi resonance (H_2O) and without any vibrational coupling (HOD in D_2O). The data are reproduced from refs 16 and 17, respectively. (c) Measured IR and Raman spectra. The data are reproduced from ref 18. (d) Computed IR spectra of the H−O−H bending vibration based on the frequency-mapping technique, including the intermolecular intramode coupling (H_2O) and without any vibrational couplings (dilute H_2O in D_2O). The data are reproduced from ref 7. All data are normalized to the peak maximum.

Table 1. Four Types of Vibrational Couplings of the O−H Stretch Vibration and the Impact of Isotope Dilution (in Red Font)
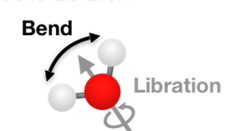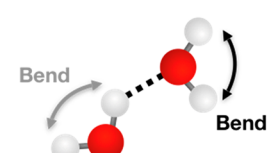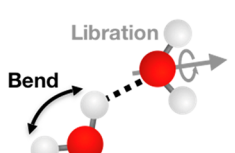

Next, we turn our attention to the vibrational dynamics of liquid water, which plays an important role in chemical

> The lineshape of the bending mode is less sensitive to vibrational coupling of water than the stretch mode, being a direct probe for hydrogen-bond network.

processes occurring in aqueous media, for example, by facilitating energy dissipation during chemical reactions.

Time-resolved spectroscopies, including pump−probe IR or two-dimensional IR (2D-IR) spectroscopy, have been used to quantify the time scales of the vibrational dynamics such as vibrational energy relaxation, orientational memory decay, and spectral diffusion.[19,20] When vibrationally exciting the O−H stretch mode, the excess vibrational energy relaxes from the O−H stretch mode to lower-frequency modes (e.g., the H−O−H bending mode at 1650 cm^{-1}, the librational mode at 600−800 cm^{-1}, and the hydrogen-bond stretch mode at 180 cm^{-1}), i.e., vibrational energy relaxation. Because the infrared excitation light is typically linearly polarized, it preferentially excites water molecules with transition dipole moments aligned along the field polarization. The decay of orientation memory, i.e., excitation anisotropy, has also been used to characterize

Table 2. Three Types of Vibrational Coupling of the H−O−H Bending Vibration and the Impact of Isotope Dilution (in Colored Font)

how the orientation of the transition dipole of the O−H stretch mode is scrambled via thermally activated rotational diffusion as well as vibrational energy transfer.[21] Spectral diffusion has been widely used to describe how quickly the O−H stretch mode loses its frequency memory, i.e., how fast the frequency of an excited oscillator is scrambled, because of the intermolecular interactions and vibrational energy transfer.[22,23]

Table 3 summarizes typical time scales for the dynamics of the O−H vibration in neat H_2O and highly diluted HDO in

Table 3. Vibrational Dynamics of the O−H Stretch Mode

	vibrational lifetime (ps)	anisotropy decay (ps)	spectral diffusion (ps)
neat H_2O	0.23 ± 0.03[23,34,35]	0.075,[22,23] 0.7,[39] <0.3[21]	<0.05,[23] 0.18[22]
HOD in D_2O	0.72 ± 0.03[36−38]	0.7,[15] 2.4,[8] <3.0−4.0[21,38,40]	0.5−1.0[37,41−43]

D_2O samples. One can see that the vibration dynamics of the O−H stretch mode is largely accelerated for neat H_2O compared with that for HDO in D_2O. For example, the anisotropy decay time in neat H_2O is >10 times faster than that of HDO in D_2O, because of the fast depolarization caused by energy transfer.[21] This acceleration of the dynamics of the O−H stretch mode arises from two mechanisms.[24] One is the vibrational energy transfer from one O−H stretch mode to other O−H stretch modes. Because the orientations of these O−H groups are rarely identical, this energy transfer will lead to depolarization of the excitation. The other mechanism is the delocalization of the O−H stretch mode in neat H_2O. The

vibrational excitation is delocalized over several neighboring O−H groups. This orientation of the transition dipole moment for the delocalized mode can be easily modulated by the conformational fluctuation of the neighboring water molecules.

In comparison to the O−H stretch mode, the vibrational dynamics of the H−O−H bending mode have been much less investigated. In Table 4, we summarize the previously reported time scales for the bending mode dynamics of H_2O in neat H_2O and H_2O in D_2O. Multiple studies have identified a vibrational lifetime of 170−260 fs for the H−O−H bending mode in pure H_2O.[18,25−27] Noticeably, the time scale of the H−O−H bending mode energy relaxation is comparable with respect to the O−H stretch mode energy relaxation of pure water. The ultrafast energy relaxation of the O−H stretch (H−O−H bending mode) has been explained by the strong intramolecular coupling attributed to the vibrational frequency matching between the O−H stretch (H−O−H bending) mode and the overtone of the H−O−H bending (librational) mode. Because the bending mode frequency is reduced from 1650 to 1450 cm^{-1}, going from H−O−H bending to H−O−D bending, increasing the frequency mismatch between the O−H stretch and the bend overtone results in weakening the intramolecular intermode coupling between O−H stretch and H−O−D bending modes. Hence, it is expected that, upon the isotopically dilution of water, the vibrational energy relaxation of the O−H stretch mode slows down because of this reduced coupling. Indeed, the vibrational relaxation of the O−H stretch mode is slower by a factor of 3 for HDO in D_2O compared to pure H_2O.

Table 4. Vibrational Dynamics of the H−O−H Bending Mode

	vibrational lifetime (ps)		anisotropy decay (ps)		spectral diffusion (ps)	
	exptl	sim	exptl	sim	exptl	sim
neat H_2O	0.17−0.26,[25−27,30,33,44,45] 0.2[18]	0.12−0.27[28,46,47]	0.08−0.17,[26,30] 0.31[18]		0.15 ± 0.03[33a], 0.24 ± 0.08[33b]	∼0.06 and ∼0.12[32]
H_2O in D_2O	0.17−0.27[18]		0.3−0.4[18]			

[a]Centerline slope method. [b]Integrated photon-echo peak shift.

In contrast, isotopic dilution of water has a smaller effect on the frequency mismatch between the H−O−H bending mode and the overtone of the librational mode, and this intramolecular intermode coupling remains largely unchanged. Hence, one can expect the vibrational energy relaxation of the H−O−H bending mode to be insensitive to the isotopic dilution. This is also borne out by experiment: we found that the vibrational lifetime of the H−O−H bending model is invariant to the isotopic composition, with a time scale of ~200 fs.[18] This fast vibrational energy relaxation of the bending mode arises from the ultrafast energy transfer of the bending mode to the higher-frequency side of the librational motion.[28]

To obtain the orientational memory dynamics, transient spectra at different polarization combinations are recorded to determine the anisotropy decay.[2] The anisotropy decay traces of the H−O−H bending mode for various H_2O/D_2O concentration ratios are shown in Figure 3a. These results
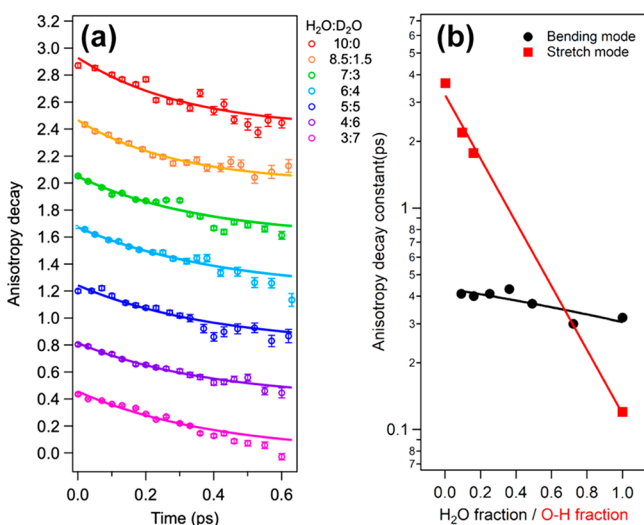

Figure 3. (a) Anisotropy decay for various H_2O/D_2O mixture. The hot ground state was subtracted from the transient absorption signal. Traces are offset by increments of 0.4. Symbols show experimental data, and solid lines show fits using a single-exponential decay. (b) Comparison of the anisotropic decay times for the bending mode and the stretch mode as a function of $H_2O/O−H$ fraction. The stretch mode data were taken from ref 21. Both bending and stretching mode data are approximated by single exponentials. The lines serve to guide the eye. The bending mode data are reprinted from ref 18.

indicate that the anisotropy decay dynamics of the H−O−H bending mode are less sensitive to the H_2O/D_2O concentration. This is in sharp contrast to the anisotropy decay of the O−H stretch mode, which is >10 times faster in neat H_2O compared to isotopically diluted water. Figure 3b summarizes these vastly different dynamics, showing the time scale of the anisotropy decay of the stretching and bending modes versus H_2O concentration.

The orientation of the transition dipole moments associated with the bending and stretch modes are aligned, roughly, along the bisector axis of the H−O−H angle and the O−H axis, respectively. As such, for sufficiently low OH concentrations, for which energy transfer is negligible, the anisotropy decay of the two modes reflects the reorientational motion of water along those two molecular coordinates. From simulations and experiments, the decay of the rotational correlation function of

the bisector axis and the O−H axis of water are known to be very similar, with a decay time of 1.5−2 ps.[29] This time constant is similar to the time constant of the anisotropy decay when pumping and probing the O−H stretch mode of isolated HDO in D_2O, while the anisotropy decay when pumping and probing the H−O−H bending mode is much faster than 1.5−2 ps. Currently, this is understood as the mixing of the bending mode and other vibrational modes; because of strong vibrational mixing,[18,22,30,31] the orientation of the transition dipole moment is rapidly randomized. As such, the anisotropy decay of the bending mode is much faster than the actual molecular reorientation, even for isotopically diluted water.

Finally, we discuss the spectral diffusion of the bending mode. 2D-IR spectroscopy can provide the time scale of the spectral diffusion, reflecting the memory loss of the excitation frequency. So far, only a few studies have been done to understand the spectral diffusion of the bending vibration.[30,32,33] Figure 4 displays the 2D-IR spectra of the H−O−H bending mode in neat H_2O obtained from experiments and simulation. The 2D spectra commonly show a positive ground-state bleach of the $1 \rightarrow 0$ transition at $\omega_3 = $ ~1630−1650 cm^{-1} and a negative excited-state absorption of the $1 \rightarrow 2$ transition at ~1550−1600 cm^{-1}. At the waiting time of 0.1 ps, all the 2D-IR spectra show a positive peak similarly elongated along the diagonal line, and the spectra become parallel to the probe axis at 0.4−0.5 ps. The time evolution of the central line slope (CLS) of the positive peak measures the memory loss of the pumping frequency. The simulation and experimental data are in good agreement, with time constants of 120 and 150 fs, respectively.[32,33] Simulation have attributed this rapid spectral diffusion to a strong intramolecular intermode coupling of the bending mode to the O−H stretch mode and low-frequency mode.[32]

A question here is to what extent the isotopic dilution impacts the spectral diffusion. Kuroda and co-workers have compared the spectral diffusion dynamics in the 2D-IR measurement for the H−O−H bending mode in neat H_2O and the H−O−D bending mode in isotopically diluted water.[33] They found that the H−O−D bending mode in isotopically diluted water and the H−O−H bending mode in neat H_2O show similar peak shift dynamics of the 2D-IR spectra with the time constant of 0.3 ± 0.05 ps and 0.24 ± 0.08 ps, respectively. This indicates that the water bending mode is almost insensitive to the intermolecular intramode coupling.

> The intramolecular intermode coupling of the bending mode of water is much stronger than its intermolecular intramode coupling.

The hydrogen-bond structure at the air−water interface has been studied by vibrational sum-frequency generation (VSFG) spectroscopy over the past two decades. Because of the optical selection rule of SFG, the SFG signal arises only from the interface where inversion symmetry is broken, i.e., not from isotropic bulk water. Because SFG signal is resonantly enhanced by interfacial vibrational transitions, it can provide vibrational and structural information on specifically interfacial water. This region is limited to the topmost few layers of water at the water−air interface.[3]
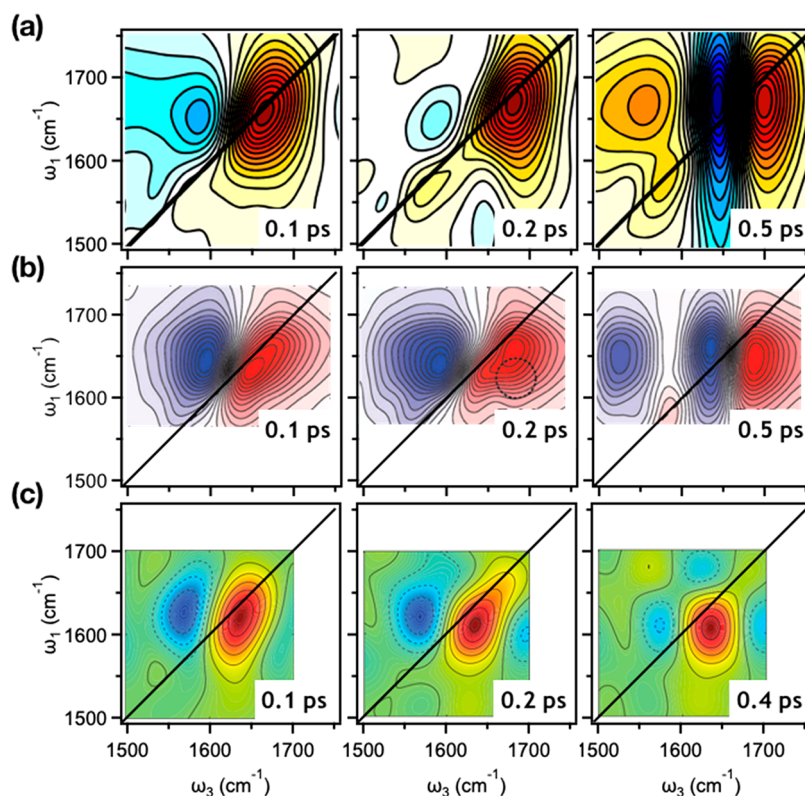
Figure 4. 2D-IR spectra in the H−O−H bending mode region as a function of waiting time for pure H_2O. (a) Experimental data of Tokmakoff and co-workers (Reproduced with permission from ref.[30] Copyright 2017 AIP Publishing), (b) experimental data of Kuroda and co-workers (Reproduced with permission from ref 33. Copyright 2014 the Royal Society of Chemistry.), and (c) simulation data of Saito and co-workers (Reproduced with permission from ref 32. Copyright 2013 AIP publishing.). The ω_1 and ω_3 indicates pump and probe frequencies, respectively.
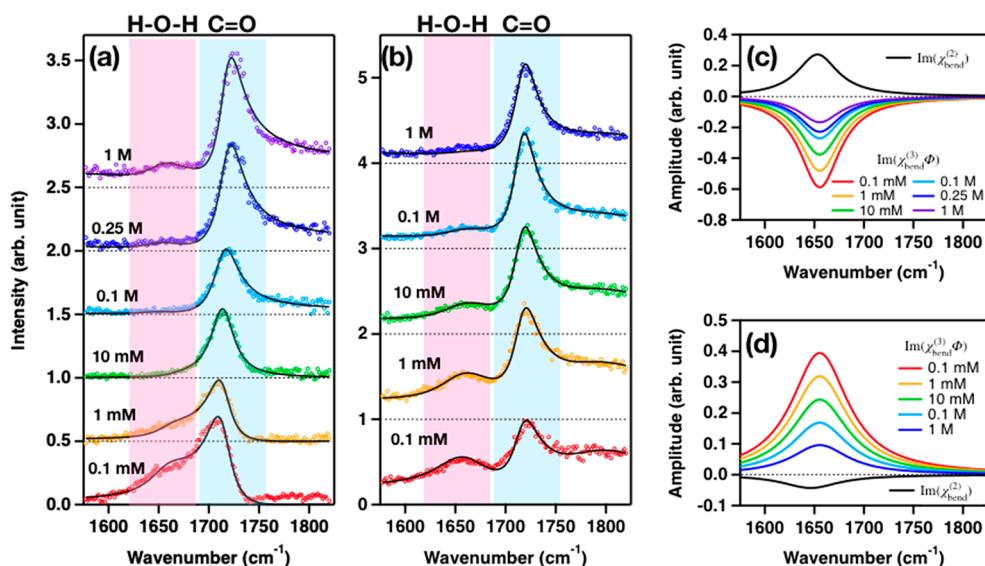

Figure 5. (a, b) SFG spectra at the (a) negatively charged (H_2O/DPPG) and (b) positively charged (H_2O/DPTAP) interfaces with various ion concentrations at ssp polarization combination (s-, s-, and p-polarization for the SFG signal, visible pulse, and IR pulse, respectively). The black lines represent the fit. The pink and blue shaded regions indicate H−O−H bending mode and C=O stretch mode contributions, respectively. (c, d) The interfacial $\mathrm{Im}(\chi^{(2)}_{bend})$ (black line) and the bulk $\mathrm{Im}(\chi^{(3)}_{bend}\Phi(c))$ (colored lines) spectra obtained from the fit of the spectra for the (c) water/DPPG and (d) water/DPTAP interfaces. The data were reproduced with permission from ref 56. Copyright 2019 American Chemical Society.

The first SFG intensity spectrum (the square of the effective surface nonlinear susceptibility, $|\chi^{(2)}_{eff}|^2$) of the bending mode at the air−water interface was experimentally measured in 2012,[48] and then the imaginary part of the SFG susceptibility, $(\mathrm{Im}(\chi^{(2)}_{bend}))$, was reported.[13] This $\mathrm{Im}(\chi^{(2)}_{bend})$ spectrum shows a

positive band. In contrast, MD simulations show that the imaginary part of the bending mode SFG spectrum exhibits both positive and negative features.[7,11,49] Tahara and co-workers attributed this discrepancy of the experimentally measured and simulated $\mathrm{Im}(\chi^{(2)}_{bend})$ to the bulk quadrupole

contribution; the simulation had assumed that the SFG signal arises solely from the interface because the interfacial dipole contribution is stronger than the bulk quadrupole contribution (electric dipole approximation),[50] while the experimental data may contain not only the leading contribution of the interfacial dipole but also contributions from the bulk quadrupole.[51] If the bulk quadrupole indeed dominates the bending mode signal, there is no chance to extract the interfacial water contribution from the SFG bending mode signal.

To explore the origin of the water SFG bending signal, one can take advantage of the fact that the sign of the $Im(\chi^{(2)}_{bend})$ SFG signal will change if the transition dipole moment flips its orientation along with the interfacial water molecules themselves. On the other hand, if the bending mode signal is governed by the proposed bulk quadrupole contribution, the sign of the $Im(\chi^{(2)}_{bend})$ will remain unchanged upon flipping the orientation of the interfacial water molecules.[51] By identifying the negative/positive change of $Im(\chi^{(2)}_{bend})$ upon going from a positively to a negatively charged interface,[52] one could elucidate whether $Im(\chi^{(2)}_{bend})$ arises from interfacial water or from bulk water.

As the presence of surface charge will induce the formation of the electrical double layer (EDL), the obtained SFG signal, $\chi^{(2)}_{eff}$, originates from two contributions: one arises from the water molecules interacting with surface molecules in the Stern layer, $\chi^{(2)}_{stern}$, while the other originates from the water molecules which can flip their orientations in response to the surface electric field in diffuse layer, $\chi^{(2)}_{Diffuse}$. Thus, extracting the $\chi^{(2)}_{Diffuse}$ contribution from the $\chi^{(2)}_{eff}$ spectrum is needed in order to address the sign of the change of the $Im(\chi^{(2)}_{bend})$. The $\chi^{(2)}_{Diffuse}$ is strongly dependent on the degree of screening of the surface charge by electrolytes in solution and therefore depends on ion concentration c. The overall response can be approached by[53−55]

$$\chi^{(2)}_{eff} = \chi^{(2)}_{Stern} + \chi^{(2)}_{Diffuse}(c) = \chi^{(2)}_{bend} + \chi^{(3)}_{bend}\Phi(c)\frac{\kappa(c)}{\kappa(c) - i\Delta k_z}$$
(4)

where $\Phi(c)$, $\kappa(c)$, and Δk_z denote the surface potential, the inverse of the Debye length, and the mismatch of the wavevectors along the surface normal (z-axis) in the reflected SFG configuration, respectively.

We measured the SFG intensity ($|\chi^{(2)}_{eff}|^2$) spectra by varying the ion concentrations, which are displayed in Figure 5a,b. Note that the spectral shape may be affected by beam geometries (Fresnel factors). The SFG spectra at the water-charged lipids interface showed a sharp C=O stretch peak at ∼1710 cm^{-1} and the bending mode peak at ∼1650 cm^{-1}. These spectra show that the interference between the 1710 cm^{-1} C=O stretch peak and the 1650 cm^{-1} water bend peak is different for the positively and negatively charged interfaces. By obtaining complex $\chi^{(2)}_{eff}$ from a Lorentzian fit of the SFG intensity and subsequently disentangling Stern and diffuse layer contributions from $\chi^{(2)}_{eff}$ via eq 4, one can obtain the $Im(\chi^{(2)}_{bend})$ and $Im(\chi^{(3)}_{bend}\Phi(c))$ spectra where $\chi^{(2)}_{Stern} \cong \chi^{(2)}_{bend}$ in our notation and $\frac{\kappa(c)}{\kappa(c) - i\Delta k_z} \cong 1$. These spectra at the negatively and positively charged interfaces are displayed in Figure 5c,d. The opposite sign of the $Im(\chi^{(2)}_{bend})$ response for the positively and negatively charged interfaces manifests that the bending mode contribution arises from the interfacial water molecules.

The SFG bending mode can provide information on the interfacial hydrogen-bond network.

Having established that the bending mode signal arises from interfacial water molecules, we further confirm that the vibrational spectral response $Im(\chi^{(2)}_{bend})$ is insensitive to the isotope composition, as established for the bending mode of bulk water. Figure 6a displays the variation of the SFG
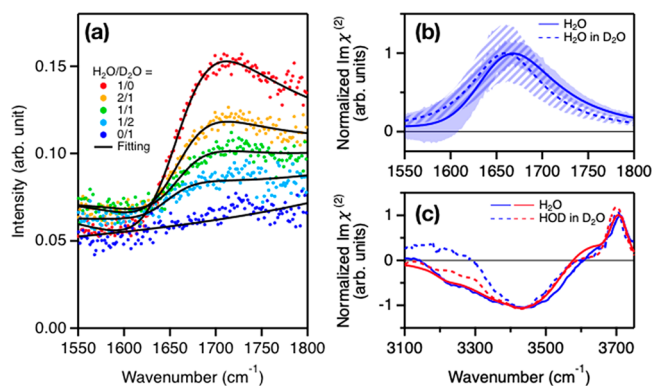

Figure 6. (a) SFG intensity spectra of the H−O−H bending mode at the water−air interface with 1/0, 2/1, 1/1, 1/2, and 0/1 H_2O/D_2O mixtures at ssp polarization combination. Solid lines are fits to the data. The data are reprinted from ref 10 by permission of the PCCP Owner Societies. (b) Normalized $Im(\chi^{(2)}_{bend})$ spectra of neat H_2O and H_2O in D_2O at the water−air interface. The data are constructed from the fits of the SFG intensity spectra in panel a. The dashed line data is obtained from $[H_2O]$ = 25%. The solid and striped shaded regions indicate the uncertainty of each measurement.[10,56] (c) Normalized $Im(\chi^{(2)}_{str})$ spectra of neat H_2O and HOD in D_2O at the water−air interface. The data are reproduced from refs 57 (blue) and 59 (red). The dashed line data is obtained from an H_2O/D_2O mixture with $[OH]$ = 25%.

intensity spectra at the water−air interface by varying the H_2O/D_2O concentration. Even the pure D_2O spectrum, which does not have any resonances in the displayed frequency region, has tilted features, which is the signature of the tail of the O−D stretch mode (∼2400 cm^{-1}). The non-negligible contribution from the O−D stretch mode implies that the bending mode SFG signal is much weaker than the stretch mode SFG signal.

By fitting the intensity spectra with a Lorentzian model, we obtain the $Im(\chi^{(2)}_{bend})$ response of the bending mode (Figure 6b).[10] The spectra show that the isotopically diluted water and neat H_2O data are similar within the error, which is in line with the bending mode of bulk water, discussed above. A relatively large deviation at ∼1600 cm^{-1} between refs 10 and 56 indicates that capturing the bending mode signal is still challenging. One can compare these bending mode SFG spectra with the O−H stretch mode SFG spectra. To have a coherent discussion about the bending mode of bulk water, we show the O−H stretch mode $Im(\chi^{(2)}_{str})$ spectra upon isotopic dilution in Figure 6c. The spectra differ slightly for reports from different groups.[57−59] So far, a commonly observed feature in the $Im(\chi^{(2)}_{str})$ spectra is the reduced low-frequency side of the negative peak around 3300 cm^{-1} and the 3600 cm^{-1} positive shoulder peak upon the isotope dilution. As a result, the isotopic dilution alters the lineshape of the O−H stretch

SFG spectra, unlike the bending mode SFG spectra. This further demonstrates that the use of the bending mode is beneficial to identify the aqueous interfacial structure without isotopically diluting water.

Above, we have described the vibrational nature of the water bending mode in the IR, Raman, and SFG spectra, in comparison with the water stretch mode. We have shown that the bending mode is insensitive to the intermolecular intramode (bending mode−bending mode) vibrational coupling, allowing us to connect the vibrational spectra with the net water structure in the aqueous system, without isotope dilution. What have the recent studies clarified using the bending mode probe? Here, we pick two examples: a study of the microscopic structure of alcohol−water binary mixtures and a study of water at protein−water interfaces. Both examples make use of the fact that the H−O−H bending mode arises solely from water molecules with no interference from other modes, unlike the O−H stretch mode for which alcohol and biomolecules also contribute. Thus, the observation based on the bending mode can provide clear evidence of the water contribution for these samples.

First, we focus on the water−alcohol mixtures, a model system of hydrophobic hydration. Water molecules surrounding a hydrophobic moiety of a molecule have been proposed to form tetrahedral or cluster-like structures,[60] which may explain the unique properties of water−alcohol mixtures, such as enhanced heat capacity. To clarify to what extent the water hydrogen-bond network in water−alcohol mixtures varies with changing the temperature, the IR spectra of the water bending mode have been measured for various water−alcohol mixtures.[61]

Figure 7 displays temperature-dependent IR spectra of the water bending mode in various water−alcohol mixtures. The

data show that increasing temperature induces a red-shift of the H−O−H bending mode frequency. As is accounted for in Figure 1, the red-shift of the bending mode frequency means that the hydrogen-bond of water is weakened. As a result, the IR spectra show that the hydrogen-bond strength of water is weakened at elevated temperatures. The interesting point is that the red-shift of the bending mode peak frequency upon increasing temperature amounts to only 0.05 cm^{-1}/°C for pure water, while it is 0.38 cm^{-1}/°C on average for alcohol−water mixtures. Furthermore, alcohols with longer alkyl chains tend to induce a larger frequency shift, indicating a more substantial weakening induced by temperature for longer alkyl chains. The observation that the hydrogen-bond strength of water is stronger in the presence of alcohol than in the pure water is linked with the enhanced heat capacity of the water−alcohol mixture.[62] Owing to the interference of the different O−H stretch modes of alcohols and water, this information cannot be obtained from the O−H stretch response. As such, the bending mode spectroscopy unraveled the variation of the hydrogen-bond network in the water−alcohol mixture.

The second example is the protein−water interface, where the O−H stretch mode of the protein side chain cannot be disentangled from the water O−H stretch mode contribution. Furthermore, the N−H stretch mode may complicate the interpretation of the O−H stretch mode spectra, because the N−H and O−H stretch frequencies overlap substantially. The H−O−H bending mode can circumvent the first problem, but the H−O−H bending mode may be masked by the very strong amide I mode at almost the same frequency. Instead, one can use the H−O−D bending mode (~1460 cm^{-1})[63] because the amide II mode (1480−1570 cm^{-1}) only weakly contributes at this frequency region because of the small Raman cross section of the amide II mode.[64]

We extracted the net water contribution at the human serum albumin (HSA) protein−water interface using the H−O−D bending mode. The SFG intensity spectra are displayed in Figure 8a, while Figure 8b shows the Im($\chi^{(2)}_{bend}$) spectra obtained through the Lorentzian model fit (black lines in panel a). The H−O−D bending mode contribution (see shaded region in Figure 8b) varies upon changing the isotope composition. The variation of the amplitude shows excellent agreement with the H−O−D concentration inferred from an equation of $[HOD]^2/[H_2O][D_2O] = 3.86$[65−67] (Figure 8c), confirming the peak assignment. The H−O−D bending mode contribution exhibits substantially higher peak frequency in the presence of HSA (~1510 cm^{-1}) than for bulk water (~1460 cm^{-1}). This indicates that interfacial water molecules near the HSA protein are more strongly hydrogen-bonded than water in the bulk. This observation seems to be linked with the fact that the HSA protein has a negatively charged site, which strongly modulates the hydrogen-bond strength of the interfacial water. As such, the water bending mode spectroscopy opens a path to extract information on water in bulk and at interfaces from the vibrational spectra of complex aqueous solutions.

In summary, we have presented new insights into the nature of water's bending mode and recent advancements in static and time-resolved water bending mode spectroscopy. We have demonstrated that the bending mode static spectral feature and also the vibrational dynamics can report directly on the hydrogen-bonded network, as the bending mode is sensitive to hydrogen bonding yet not obscured by intermolecular vibrational coupling effects. This makes the bending mode an excellent complement to the O−H stretch mode, which has
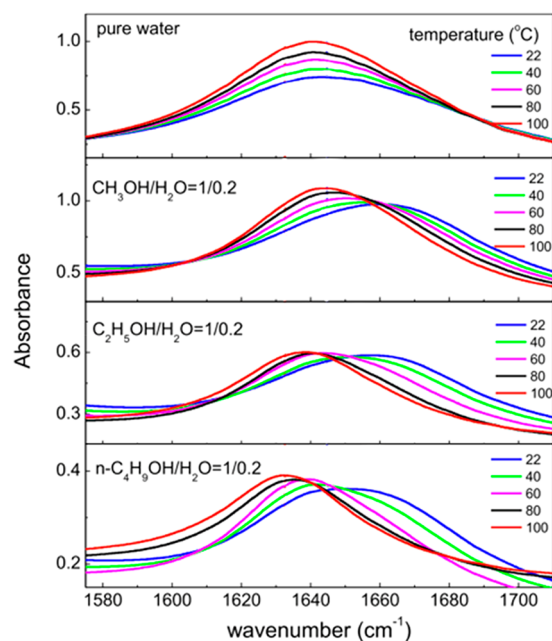

Figure 7. IR spectra in the water bending mode range of alcohol−water mixtures at various temperatures. These solutions have the same composition of 1/0.2 molar ratio (alcohol/water). The legend indicates the temperature of the system in units of °C. The data is reproduced with permission from ref 61. Copyright 2019 American Chemical Society.
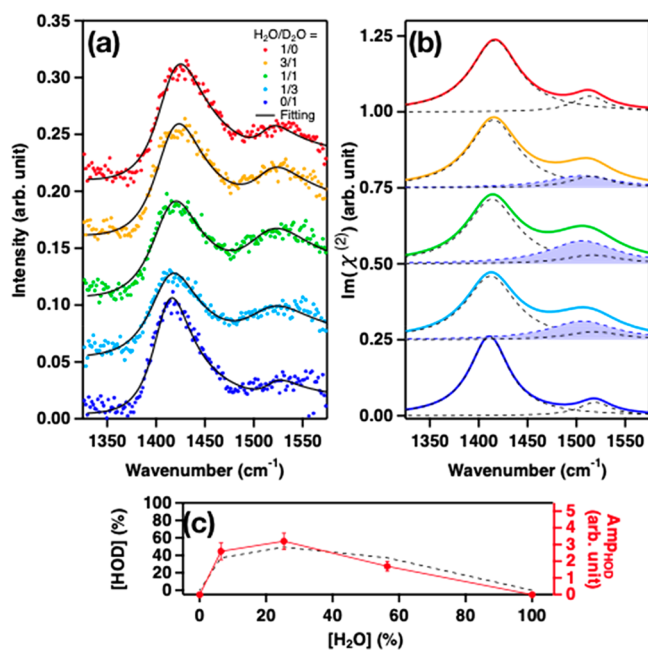
Figure 8. (a) The H−O−D bending mode spectra at HSA−water interface with various H_2O/D_2O mixture ratios. (b) The $Im(\chi^{(2)})$ spectra of HSA and water contributions from the fits (solid lines in panel a). Shaded regions in blue represent the H−O−D bending mode contributions of isotopically diluted water. (c) Amplitude of the H−O−D contribution vs H_2O fraction. Theoretical prediction denoted by the black broken line is obtained from the equation of $[HOD]^2/[H_2O][D_2O] = 3.86$.[65−67] These data are reproduced from ref 10 by permission of the PCCP Owner Societies.

> The water bending mode can decode the net water contribution from various complex aqueous systems such as water−liquid mixture and solid−water and protein−water interfaces.

been traditionally studied as a reporter of the microscopic structure and dynamics of water's hydrogen-bond network, and for which intermolecular vibrational coupling effects do play a role.

Several fundamental properties of the bending mode remain unknown. The vibrational properties of the bending mode in ice are not well understood.[68] Even though time-resolved vibrational spectroscopy in the bulk has revealed the vibrational dynamics to be insensitive to the local molecular environments for bulk liquid water, this observation may not apply to interfacial water. Time-resolved surface vibrational spectroscopy needs to be carried out to explore the energy transfer of bending mode excitation at the air−water (ice) interface to understand the energy flow at the interface. Bending mode spectroscopy can further provide a powerful way to (re)explore the microscopic hydrogen-bond network of various aqueous systems, which can be applied to further understand complicated phenomena such as liquid−liquid phase separation or hydrogen-evolution reactions at the surface of catalysts *in situ*/*operando*.

■ AUTHOR INFORMATION

Corresponding Authors
   Yuki Nagata − *Max Planck Institute for Polymer Research, 55128 Mainz, Germany;* orcid.org/0000-0001-9727-6641; Email: nagata@mpip-mainz.mpg.de
   Mischa Bonn − *Max Planck Institute for Polymer Research, 55128 Mainz, Germany;* orcid.org/0000-0001-6851-8453; Email: bonn@mpip-mainz.mpg.de

Authors
   Takakazu Seki − *Max Planck Institute for Polymer Research, 55128 Mainz, Germany*
   Kuo-Yang Chiang − *Max Planck Institute for Polymer Research, 55128 Mainz, Germany*
   Chun-Chieh Yu − *Max Planck Institute for Polymer Research, 55128 Mainz, Germany*
   Xiaoqing Yu − *Max Planck Institute for Polymer Research, 55128 Mainz, Germany*
   Masanari Okuno − *Department of Basic Science, Graduate School of Arts and Sciences, The University of Tokyo, Meguro, Tokyo 153-8902, Japan;* orcid.org/0000-0002-3682-9350
   Johannes Hunger − *Max Planck Institute for Polymer Research, 55128 Mainz, Germany;* orcid.org/0000-0002-4419-5220

Complete contact information is available at:
https://pubs.acs.org/10.1021/acs.jpclett.0c01259

Author Contributions
#T.S. and K.-Y.C. contributed equally.

Notes
The authors declare no competing financial interest.

Biographies

Takakazu Seki received his M.S. in chemistry at University of Tokyo, Japan in 2014 and his doctorate at Tokyo Institute of Technology, Japan in 2019. After that, he joined the Max Planck Institute for Polymer Research (MPI-P), Mainz, Germany as a postdoctoral fellow, and his current research focus is on interfacial water behaviors explored by SFG spectroscopy.

Kuo-Yang Chiang is a Ph.D. student at the MPI-P, Mainz, Germany. He received his Physics masters degree in 2016 from National Central University (NCU) and stayed at Academia Sinica, Taipei, Taiwan. He joined the MPI-P as a Ph.D. candidate in 2019. His research focuses on the structure and vibrational dynamics of interfacial water by SFG spectroscopy.

Chun-Chieh Yu obtained his M.S, in Molecular Science, Applied Chemistry at National Chiao Tung University, Taiwan in 2018. He is currently pursuing a Ph.D. degree at the MPI-P, Mainz, Germany. His research interests are focused on the nonlinear spectroscopy of water including SFG and hyper-Raman spectroscopy.

Xiaoqing Yu obtained her M.S. in Materials Science and Engineering at Beijing University of Chemical Technology, Beijing, China in 2018. She is currently a Ph.D. student at the MPI-P, Mainz, Germany. Her research interests are interfacial water structure at static and dynamic interfaces.

Masanari Okuno is an associate professor at the University of Tokyo, Tokyo, Japan. He received his Ph.D. in 2012 from the University of Tokyo. After postdoctoral research at MPI-P, he became an assistant professor at University of Tsukuba in 2013. He joined the University of Tokyo in 2019. His research focus is vibrational spectroscopy of the molecular structure and intermolecular interaction in liquids and solutions.

Johannes Hunger is a group leader at the MPI-P, Mainz, Germany. He received his Ph.D. in 2010 from the University of Regensburg, Germany. After his postdoctoral stay at the FOM Institute AMOLF, Netherlands, he joined the MPI-P in 2012. His research interests are centered around the dynamics of liquids with a focus on hydrogen-bonding and Coulombic interactions.

Yuki Nagata is a group leader at the MPI-P, Mainz, Germany. He received his Ph.D. in 2007 from Kyoto University. After his stay at BASF SE and the University of California, Irvine, he joined MPI-P in 2011. His research focus is on the theoretical modeling and experiment of vibrational spectroscopy.

Mischa Bonn is a director at MPI-P, Mainz, Germany. He received his Ph.D. in 1996 from the University of Eindhoven, The Netherlands. After postdoctoral research at the Fritz Haber Institute and Columbia University, he worked at Leiden University. In 2004 he became a group leader at AMOLF, Amsterdam, The Netherlands. In 2011 he joined MPI-P. His research interests are the structure and dynamics of molecules at interfaces and electron transfer across interfaces.

■ ACKNOWLEDGMENTS

■ REFERENCES

(1) Ball, P. Water as an Active Constituent in Cell Biology. *Chem. Rev.* **2008**, *108*, 74−108.

(2) Bakker, H. J.; Skinner, J. L. Vibrational Spectroscopy as a Probe of Structure and Dynamics in Liquid Water. *Chem. Rev.* **2010**, *110*, 1498−1517.

(3) Shen, Y. R.; Ostroverkhov, V. Sum-Frequency Vibrational Spectroscopy on Water Interfaces: Polar Orientation of Water Molecules at Interfaces. *Chem. Rev.* **2006**, *106*, 1140−1154.

(4) Rey, R.; Møller, K. B.; Hynes, J. T. Hydrogen Bond Dynamics in Water and Ultrafast Infrared Spectroscopy: A Theoretical Study. *J. Phys. Chem. A* **2002**, *106*, 11993−11996.

(5) Ojha, D.; Karhan, K.; Kühne, T. D. On the Hydrogen Bond Strength and Vibrational Spectroscopy of Liquid Water. *Sci. Rep.* **2018**, *8*, 16888.

(6) Falk, M. The Frequency of the H-O-H Bending Fundamental in Solids and Liquids. *Spectrochim. Acta* **1984**, *40*, 43−48.

(7) Ni, Y.; Skinner, J. L. IR and SFG Vibrational Spectroscopy of the Water Bend in the Bulk Liquid and at the Liquid-Vapor Interface, Respectively. *J. Chem. Phys.* **2015**, *143*, 014502.

(8) Perakis, F.; De Marco, L.; Shalit, A.; Tang, F.; Kann, Z. R.; Kühne, T. D.; Torre, R.; Bonn, M.; Nagata, Y. Vibrational Spectroscopy and Dynamics of Water. *Chem. Rev.* **2016**, *116*, 7590−7607.

(9) Maréchal, Y. IR Spectroscopy of an Exceptional H-Bonded Liquid: Water. *J. Mol. Struct.* **1994**, *322*, 105−111.

(10) Seki, T.; Yu, C.-C.; Yu, X.; Ohto, T.; Sun, S.; Meister, K.; Backus, E. H. G.; Bonn, M.; Nagata, Y. Decoding the Molecular Water Structure at Complex Interfaces through Surface-Specific Spectroscopy of the Water Bending Mode. *Phys. Chem. Chem. Phys.* **2020**, *22*, 10934−10940.

(11) Nagata, Y.; Hsieh, C.-S.; Hasegawa, T.; Voll, J.; Backus, E. H. G.; Bonn, M. Water Bending Mode at the Water-Vapor Interface Probed by Sum-Frequency Generation Spectroscopy: A Combined Molecular Dynamics Simulation and Experimental Study. *J. Phys. Chem. Lett.* **2013**, *4*, 1872−1877.

(12) Dutta, C.; Benderskii, A. V. On the Assignment of the Vibrational Spectrum of the Water Bend at the Air/Water Interface. *J. Phys. Chem. Lett.* **2017**, *8*, 801−804.

(13) Kundu, A.; Tanaka, S.; Ishiyama, T.; Ahmed, M.; Inoue, K.; Nihonyanagi, S.; Sawai, H.; Yamaguchi, S.; Morita, A.; Tahara, T. Bend Vibration of Surface Water Investigated by Heterodyne-Detected Sum Frequency Generation and Theoretical Study: Dominant Role of Quadrupole. *J. Phys. Chem. Lett.* **2016**, *7*, 2597−2601.

(14) Ford, T. A.; Falk, M. Hydrogen Bonding in Water and Ice. *Can. J. Chem.* **1968**, *46*, 3579−3586.

(15) Hu, Q.; Zhao, H.; Ouyang, S. Understanding Water Structure from Raman Spectra of Isotopic Substitution H_2O/D_2O up to 573 K. *Phys. Chem. Chem. Phys.* **2017**, *19*, 21540−21547.

(16) Kananenka, A. A.; Skinner, J. L. Fermi Resonance in OH-Stretch Vibrational Spectroscopy of Liquid Water and the Water Hexamer. *J. Chem. Phys.* **2018**, *148*, 244107.

(17) Auer, B. M.; Skinner, J. L. IR and Raman Spectra of Liquid Water: Theory and Interpretation. *J. Chem. Phys.* **2008**, *128*, 224511.

(18) Yu, C.-C.; Chiang, K.-Y.; Masanari, O.; Seki, T.; Ohto, T.; Yu, X.; Zhong, K.; Korepanov, V.; Hamaguchi, H.; Bonn, M.; Hunger, J.; Nagata, Y. Vibrational Couplings and Energy Transfer Pathways of Water's Bending Mode. *ChemRxiv* **2020** DOI: 10.26434/chemrxiv.12640760.v1.

(19) Mukamel, S. *Principles of Nonlinear Optical Spectroscopy*; Oxford University Press, 1999.

(20) Laage, D.; Stirnemann, G.; Sterpone, F.; Rey, R.; Hynes, J. T. Reorientation and Allied Dynamics in Water and Aqueous Solutions. *Annu. Rev. Phys. Chem.* **2011**, *62*, 395−416.

(21) Woutersen, S.; Bakker, H. J. Resonant Intermolecular Transfer of Vibrational Energy in Liquid Water. *Nature* **1999**, *402*, 507−509.

(22) Ramasesha, K.; De Marco, L.; Mandal, A.; Tokmakoff, A. Water Vibrations Have Strongly Mixed Intra- and Intermolecular Character. *Nat. Chem.* **2013**, *5*, 935−940.

(23) Cowan, M. L.; Bruner, B. D.; Huse, N.; Dwyer, J. R.; Chugh, B.; Nibbering, E. T. J.; Elsaesser, T.; Miller, R. J. D. Ultrafast Memory Loss and Energy Redistribution in the Hydrogen Bond Network of Liquid H_2O. *Nature* **2005**, *434*, 199−202.

(24) Nagata, Y.; Yoshimune, S.; Hsieh, C.; Hunger, J.; Bonn, M. Ultrafast Vibrational Dynamics of Water Disentangled by Reverse Nonequilibrium Ab Initio Molecular Dynamics Simulations. *Phys. Rev. X* **2015**, *5*, 021002.

(25) Lindner, J.; Vöhringer, P.; Pshenichnikov, M. S.; Cringus, D.; Wiersma, D. A.; Mostovoy, M. Vibrational Relaxation of Pure Liquid Water. *Chem. Phys. Lett.* **2006**, *421*, 329−333.

(26) Huse, N.; Ashihara, S.; Nibbering, E. T. J.; Elsaesser, T. Ultrafast Vibrational Relaxation of O-H Bending and Librational Excitations in Liquid H_2O. *Chem. Phys. Lett.* **2005**, *404*, 389−393.

(27) Ashihara, S.; Huse, N.; Espagne, A.; Nibbering, E. T. J.; Elsaesser, T. Vibrational Couplings and Ultrafast Relaxation of the O-H Bending Mode in Liquid H_2O. *Chem. Phys. Lett.* **2006**, *424*, 66−70.

(28) Imoto, S.; Xantheas, S. S.; Saito, S. Ultrafast Dynamics of Liquid Water: Energy Relaxation and Transfer Processes of the OH Stretch and the HOH Bend. *J. Phys. Chem. B* **2015**, *119*, 11068−11078.

(29) Wu, Y.; Tepper, H. L.; Voth, G. A. Flexible Simple Point-Charge Water Model with Improved Liquid-State Properties. *J. Chem. Phys.* **2006**, *124*, 024503.

(30) Carpenter, W. B.; Fournier, J. A.; Biswas, R.; Voth, G. A.; Tokmakoff, A. Delocalization and Stretch-Bend Mixing of the HOH Bend in Liquid Water. *J. Chem. Phys.* **2017**, *147*, 084503.

(31) Rey, R.; Ingrosso, F.; Elsaesser, T.; Hynes, J. T. Pathways for H_2O Bend Vibrational Relaxation in Liquid Water. *J. Phys. Chem. A* **2009**, *113*, 8949−8962.

(32) Imoto, S.; Xantheas, S. S.; Saito, S. Ultrafast Dynamics of Liquid Water: Frequency Fluctuations of the OH Stretch and the HOH Bend. *J. Chem. Phys.* **2013**, *139*, 044503.

(33) Chuntonov, L.; Kumar, R.; Kuroda, D. G. Non-Linear Infrared Spectroscopy of the Water Bending Mode: Direct Experimental

Evidence of Hydration Shell Reorganization? *Phys. Chem. Chem. Phys.* **2014**, *16*, 13172−13181.

(34) Kraemer, D.; Cowan, M. L.; Paarmann, A.; Huse, N.; Nibbering, E. T. J.; Elsaesser, T.; Miller, R. J. D. Temperature Dependence of the Two-Dimensional Infrared Spectrum of Liquid H2O. *Proc. Natl. Acad. Sci. U. S. A.* **2008**, *105*, 437−442.

(35) van der Post, S. T.; Hsieh, C.-S.; Okuno, M.; Nagata, Y.; Bakker, H. J.; Bonn, M.; Hunger, J. Strong Frequency Dependence of Vibrational Relaxation in Bulk and Surface Water Reveals Sub-Picosecond Structural Heterogeneity. *Nat. Commun.* **2015**, *6*, 8384.

(36) De Marco, L.; Ramasesha, K.; Tokmakoff, A. Experimental Evidence of Fermi Resonances in Isotopically Dilute Water from Ultrafast Broadband IR Spectroscopy. *J. Phys. Chem. B* **2013**, *117*, 15319−15327.

(37) Woutersen, S.; Emmerichs, U.; Nienhuys, H. K.; Bakker, H. J. Anomalous Temperature Dependence of Vibrational Lifetimes in Water and Ice. *Phys. Rev. Lett.* **1998**, *81*, 1106−1109.

(38) Fecko, C. J.; Loparo, J. J.; Roberts, S. T.; Tokmakoff, A. Local Hydrogen Bonding Dynamics and Collective Reorganization in Water: Ultrafast Infrared Spectroscopy of HOD/D2O. *J. Chem. Phys.* **2005**, *122*, 054506.

(39) De Marco, L.; Fournier, J. A.; Thämer, M.; Carpenter, W.; Tokmakoff, A. Anharmonic Exciton Dynamics and Energy Dissipation in Liquid Water from Two- Dimensional Infrared Spectroscopy Water from Two-Dimensional Infrared Spectroscopy. *J. Chem. Phys.* **2016**, *145*, 094501.

(40) Nienhuys, H.-K.; van Santen, R. A.; Bakker, H. J. Orientational Relaxation of Liquid Water Molecules as an Activated Process. *J. Chem. Phys.* **2000**, *112*, 8487−8494.

(41) Lascoux, N.; Gallot, G.; Hache, F.; Gale, G. M.; Bratos, S.; Leicknam, J. C. Femtosecond Dynamics of Hydrogen Bonds in Liquid Water: A Real Time Study. *J. Chin. Chem. Soc.* **2000**, *47*, 685−692.

(42) Laenen, R.; Rauscher, C.; Laubereau, A. Dynamics of Local Substructures in Water Observed by Ultrafast Infrared Hole Burning. *Phys. Rev. Lett.* **1998**, *80*, 2622−2625.

(43) Lawrence, C. P.; Skinner, J. L. Vibrational Spectroscopy of HOD in Liquid D2O. VI. Intramolecular and Intermolecular Vibrational Energy Flow. *J. Chem. Phys.* **2003**, *119*, 1623−1633.

(44) Ashihara, S.; Fujioka, S.; Shibuya, K. Temperature Dependence of Vibrational Relaxation of the OH Bending Excitation in Liquid H2O. *Chem. Phys. Lett.* **2011**, *502*, 57−62.

(45) Lindner, J.; Cringus, D.; Pshenichnikov, M. S.; Vöhringer, P. Anharmonic Bend-Stretch Coupling in Neat Liquid Water. *Chem. Phys.* **2007**, *341*, 326−335.

(46) Bastida, A.; Zúñiga, J.; Requena, A.; Miguel, B. Hybrid Quantum/Classical Simulation of the Vibrational Relaxation of the Bend Fundamental in Liquid Water. *J. Chem. Phys.* **2009**, *131*, 204505.

(47) Ingrosso, F.; Rey, R.; Elsaesser, T.; Hynes, J. T. Ultrafast Energy Transfer from the Intramolecular Bending Vibration to Librations in Liquid Water. *J. Phys. Chem. A* **2009**, *113*, 6657−6665.

(48) Vinaykin, M.; Benderskii, A. V. Vibrational Sum-Frequency Spectrum of the Water Bend at the Air/Water Interface. *J. Phys. Chem. Lett.* **2012**, *3*, 3348−3352.

(49) Moberg, D. R.; Straight, S. C.; Paesani, F. Temperature Dependence of the Air/Water Interface Revealed by Polarization Sensitive Sum-Frequency Generation Spectroscopy. *J. Phys. Chem. B* **2018**, *122*, 4356−4365.

(50) Tang, F.; Ohto, T.; Sun, S.; Rouxel, J. R.; Imoto, S.; Backus, E. H. G.; Mukamel, S.; Bonn, M.; Nagata, Y. Molecular Structure and Modeling of Water-Air and Ice-Air Interfaces Monitored by Sum-Frequency Generation. *Chem. Rev.* **2020**, *120*, 3633−3667.

(51) Shen, Y. R. Basic Theory of Surface Sum-Frequency Generation. *J. Phys. Chem. C* **2012**, *116*, 15505−15509.

(52) Nihonyanagi, S.; Yamaguchi, S.; Tahara, T. Direct Evidence for Orientational Flip-Flop of Water Molecules at Charged Interfaces: A Heterodyne-Detected Vibrational Sum Frequency Generation Study. *J. Chem. Phys.* **2009**, *130*, 204704.

(53) Wen, Y.-C.; Zha, S.; Liu, X.; Yang, S.; Guo, P.; Shi, G.; Fang, H.; Shen, Y. R.; Tian, C. Unveiling Microscopic Structures of Charged Water Interfaces by Surface-Specific Vibrational Spectroscopy. *Phys. Rev. Lett.* **2016**, *116*, 016101.

(54) Gonella, G.; Lütgebaucks, C.; De Beer, A. G. F.; Roke, S. Second Harmonic and Sum-Frequency Generation from Aqueous Interfaces Is Modulated by Interference. *J. Phys. Chem. C* **2016**, *120*, 9165−9173.

(55) Ohno, P. E.; Wang, H.; Geiger, F. M. Second-Order Spectral Lineshapes from Charged Interfaces. *Nat. Commun.* **2017**, *8*, 1032.

(56) Seki, T.; Sun, S.; Zhong, K.; Yu, C.; Machel, K.; Dreier, L. B.; Backus, E. H. G.; Bonn, M.; Nagata, Y. Unveiling Heterogeneity of Interfacial Water through the Water Bending Mode. *J. Phys. Chem. Lett.* **2019**, *10*, 6936−6941.

(57) Nihonyanagi, S.; Ishiyama, T.; Lee, T.-K.; Yamaguchi, S.; Bonn, M.; Morita, A.; Tahara, T. Unified Molecular View of the Air/Water Interface Based on Experimental and Theoretical $\chi^{(2)}$ Spectra of an Isotopically Diluted Water Surface. *J. Am. Chem. Soc.* **2011**, *133*, 16875−16880.

(58) Xu, X.; Shen, Y. R.; Tian, C. Phase-Sensitive Sum Frequency Vibrational Spectroscopic Study of Air/Water Interfaces: H_2O, D_2O, and Diluted Isotopic Mixtures. *J. Chem. Phys.* **2019**, *150*, 144701.

(59) Smit, W. J.; Versluis, J.; Backus, E. H. G.; Bonn, M.; Bakker, H. J. Reduced Near-Resonant Vibrational Coupling at the Surfaces of Liquid Water and Ice. *J. Phys. Chem. Lett.* **2018**, *9*, 1290−1294.

(60) Cheng, Y. K.; Rossky, P. J. Surface Topography Dependence of Biomolecular Hydrophobic Hydration. *Nature* **1998**, *392*, 696−699.

(61) Deng, G.-H.; Shen, Y.; Chen, H.; Chen, Y.; Jiang, B.; Wu, G.; Yang, X.; Yuan, K.; Zheng, J. Ordered-to-Disordered Transformation of Enhanced Water Structure on Hydrophobic Surfaces in Concentrated Alcohol-Water Solutions. *J. Phys. Chem. Lett.* **2019**, *10*, 7922−7928.

(62) Benson, G. C.; D'Arcy, P. J. Excess Isobaric Heat Capacities of Water-n-Alcohol Mixtures. *J. Chem. Eng. Data* **1982**, *27*, 439−442.

(63) Falk, M. Frequencies of H-O-H, H-O-D and D-O-D Bending Fundamentals in Liquid Water. *J. Raman Spectrosc.* **1990**, *21*, 563−567.

(64) Kurouski, D.; Van Duyne, R. P.; Lednev, I. K. Exploring the Structure and Formation Mechanism of Amyloid Fibrils by Raman Spectroscopy: A Review. *Analyst* **2015**, *140*, 4967−4980.

(65) Meija, J.; Mester, Z.; D'Ulivo, A. Mass Spectrometric Separation and Quantitation of Overlapping Isotopologues. H2O/HOD/D2O and H2Se/HDSe/D2Se Mixtures. *J. Am. Soc. Mass Spectrom.* **2006**, *17*, 1028−1036.

(66) Duplan, J. C.; Mahi, L.; Brunet, J. L. NMR Determination of the Equilibrium Constant for the Liquid H_2O-D_2O Mixture. *Chem. Phys. Lett.* **2005**, *413*, 400−403.

(67) Wolfsberg, M.; Massa, A. A.; Pyper, J. W. Effect of Vibrational Anharmonicity on the Isotopic Self-Exchange Equilibria H 2 X+D 2 X = 2HDX. *J. Chem. Phys.* **1970**, *53*, 3138−3146.

(68) Imoto, S.; Xantheas, S. S.; Saito, S. Molecular Origin of the Difference in the HOH Bend of the IR Spectra between Liquid Water and Ice. *J. Chem. Phys.* **2013**, *138*, 054506.